Local rules for fabricating allosteric networks

Nidhi Pashine **

Department of Physics, The University of Chicago, Chicago, Illinois 60637, USA

(Received 11 February 2021; accepted 16 June 2021; published 28 June 2021)

Mechanical properties of disordered networks can be significantly tailored by modifying a small fraction of their bonds. This procedure has been used to design and build mechanical metamaterials with a variety of responses. A long-range "allosteric" response, where a localized input strain at one site gives rise to a localized output strain at a distant site, has been of particular interest. This work presents an approach to incorporating allosteric responses in experimental systems by pruning disordered networks *in situ*. Previous work has relied on computer simulations to design and predict the response of such systems using a cost function where the response of the entire network to each bond removal is used at each step to determine which bond to prune. It is not feasible to follow such a design protocol in experiments where one has access only to local response at each site. This paper presents design algorithms that allow determination of what bonds to prune based purely on the local forces in the network without employing a cost function; using only local information, allosteric networks are designed in simulations and then built out of real materials. The results show that some pruning strategies work better than others when translated into an experimental system. A method is presented to measure local stresses experimentally in disordered networks. This approach is then used to implement pruning methods to design desired responses *in situ*. Results from these experiments confirm that the pruning methods are robust and work in a real laboratory material.

DOI: 10.1103/PhysRevMaterials.5.065607

I. INTRODUCTION

Recent advances in the field of mechanical metamaterials have shown that disordered networks are extremely tunable so that their mechanical response can be altered dramatically by modifying a small number of edges or bonds between nodes. This can be demonstrated in the Poisson's ratio ν , which is the negative of the ratio of the strain along the transverse axes to an applied strain along a given axis. In an isotropic network material in d dimensions, ν can be varied between the two theoretical limits, $\nu = -1$ (auxetic) and $\nu = +1/(d-1)$ (incompressible), by selectively removing a small fraction of the network bonds [1–3].

A more general property that can be incorporated into a disordered network is a long-distance response, where applying an input strain at a local site in the system creates an output strain at another distant localized site [4–6]. This is referred to as a mechanical "allosteric" response because it is inspired by the property of allostery in protein molecules.

Both allosteric and auxetic responses have been successfully designed and incorporated into physical networks by pruning selected bonds [4,7]. An important difference between auxetic and allosteric response is that the Poisson's ratio is a monotonic function of the ratio of the shear *G* and bulk *B* moduli of a material. In a disordered system, once contributions of every bond to the bulk and shear moduli are known, it is straightforward to change its Poisson's ratio by pruning specific bonds.

On the other hand, in earlier works, allosteric systems have been designed by removing bonds from a disordered network using a cost function. This protocol succeeds well for designing materials with multiple targets controlled by a single source using computer simulations [4,8]. A cost function calculates the global response of the system due to the removal of each bond individually in the network in order to decide what bonds need to be pruned to minimize the difference from a desired response. Such a cost function is difficult to interpret or quantify in terms of simple local properties of the individual bonds in the network. This makes it difficult to create such behavior in a network *in situ* so that the result can be achieved without recourse to prior design on a computer.

This paper takes an alternate approach for designing a pruning protocol; the aim is to use only local information encoded in the tension on each bond due to an externally applied strain. This would allow the creation of allosteric responses in spring-network simulations by using only local information before a bond is removed. This approach is a generalization of the one used to incorporate auxetic response into networks [1]. In that case, the pruning was based on the local stresses in the bonds due to an externally applied strain. In the case of allostery, the procedure is extended to include the response to a set of separate, individually applied strains which are then combined. The results are then tested and validated in experiments; I take the networks that were designed in simulations and build them out of rubber sheets.

One problem encountered in using simulated networks to prune real materials is that the simulations used, which have been of disordered central-spring networks derived from jammed packings of spheres [9], are overly simplified models

^{*}npashine@uchicago.edu

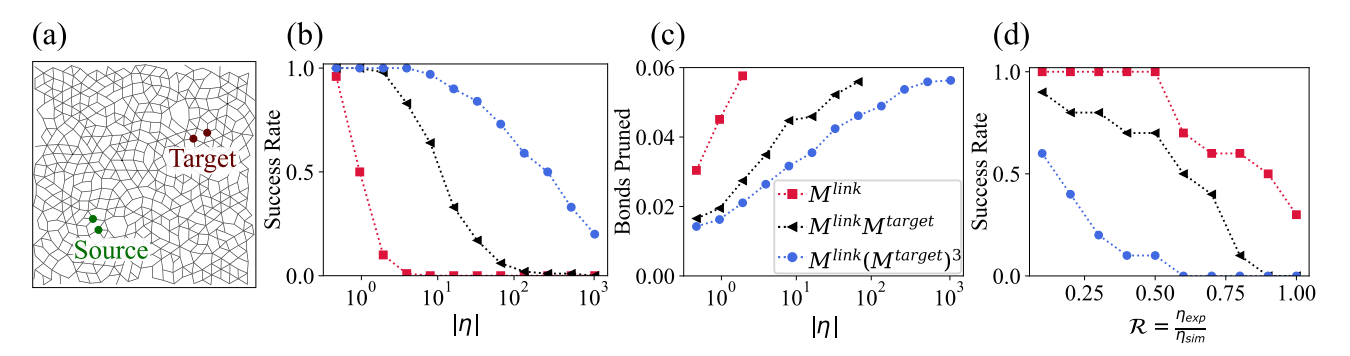


FIG. 1. (a) A sample network with adjacent nodes chosen to be source and target sites. (b) Results from pruning in simulations. Success rate of pruning networks as a function of $|\eta|$. Networks pruned to lower the effective moduli $M^{\rm eff} = M^{\rm link}(M^{\rm target})^3$ (blue circles) have the highest success rate, followed by $M^{\rm link}M^{\rm target}$ (black triangles), with $M^{\rm link}$ (red squares) being the least effective way to prune. (c) Average fraction of bonds pruned as a function of $|\eta|$ for each of the three $M^{\rm eff}$. (d) Performance of experimental networks that were designed in simulations to have $\eta \approx 1$. Plot shows the fraction of networks with a response higher than $\mathcal R$ as a function of $\mathcal R$.

of the real materials. A physical system is more complicated than such a spring network because it has forces other than those derived from harmonic central-spring interactions. To circumvent this problem, I present an experimental approach to measure the relative magnitude of stresses in networks under any external strain and use it to prune the network systems *in situ*. This is done using photoelastic networks that are observed between pairs of cross-polarizers. In this approach, no simulations are necessary for determining which bonds to prune.

I find that experimental networks that are designed in simulations have a drastically different response than those that are pruned *in situ* using photoelastic stress measurements. In addition, the different local pruning methods can produce different results in experiments even when they are designed to give the same response in simulations. Taken together, this work improves the understanding of the mechanisms that control allostery in mechanical systems and opens up possibilities of building new and interesting mechanical responses in real materials.

II. THEORETICAL APPROACH

The random disordered spring networks are created in two dimensions, 2D, with periodic boundary conditions. These networks are derived from 2D jammed packings of soft disks which are under force balance [9–11]. Each point of contact between the disks is replaced by a harmonic spring that connects the centers of the two disks. The equilibrium length of each spring is chosen to be the distance between the centers of the disks. This ensures that the resultant network of nodes connected by bonds is under zero stress in its ground state. The network coordination number, which is the average number of bonds coming out of a node, is denoted by Z. In order for such a network to be rigid, it needs to have an average $Z \geqslant Z_c$, the critical coordination number. In d dimensions and excluding finite-size effects, $Z_c = 2d$; the 2D networks used here have $Z > Z_c = 4$.

In order to incorporate a long-distance allosteric response between two distant sites within a network, two pairs of nodes are picked at random as the source and target, respectively. These are separated by typically half of the system size. One such network is shown in Fig. 1(a). In order to have an allosteric interaction, there should be an output strain ϵ_T at the target pair of nodes when an input strain ϵ_S is applied between the two source nodes. The ratio of output to input strains is $\eta \equiv \frac{\epsilon_T}{\epsilon_S}$. The aim is to incorporate an allosteric response with a desired value of η in the network by removing specific bonds from the network using a local pruning rule that uses only information that is available prior to the pruning itself.

The general idea is to apply strains at both the input and output sites (in some cases simultaneously and sometimes separately) to discover which bonds should be removed in order to produce a strain at the target when the source is activated. One might be tempted simply to minimize the energy for a specific mechanical behavior. That is, one might consider removing the bonds that are under highest stress when both the source and target are simultaneously put under the desired strains. This, however, would nearly always fail, because the dominant energy for the strained system is often just due to the strains of the source and target, irrespective of whether the source and target are applied simultaneously. In case of designing an allosteric response, the goal is not merely to lower the energy for the input and output strains but to create an interaction between the source and target sites. Thus the source and target sites must communicate with each other. In order to achieve this, one needs to identify specifically the bonds that facilitate and the ones that hinder this allosteric response. By identifying and pruning the right set of bonds, it is possible to minimize the *interaction energy* (not just the total energy of distortion) of the input and output strains.

We apply a deformation to our system, ϵ^k . This ϵ^k could be an axial strain applied between two points in the system or a combination of strains applied at various locations. In response to this applied strain ϵ^k , each bond in the system, j, is stretched or compressed. The force on bond j that appears due to ϵ^k is denoted by T_j^k . For example, T_j^{source} is defined as the force on bond j as a result of the input strain applied at the *source*. A positive value of T_j corresponds to extension, and a negative value implies compression of the spring.

Since all the calculations below are in the linear-response regime,

$$T_j^{-k} = -T_j^k; \ T_j^{k+l} = T_j^k + T_j^l.$$

One can calculate the energies in each bond of the network under any applied deformation ϵ^k : the energy U_i^k in bond j when its length is changed by an amount γ_i^k due to a force T_i^k

$$U_i^k = \frac{1}{2} T_i^k \gamma_i^k. \tag{1}$$

Since the total energy of the network is simply the sum of the energies of all the individual springs, the total energy stored in the network under an applied strain ϵ^k is $U^k = \sum_i U_i^k$.

The modulus M^k for any given deformation ϵ^k is defined as $U^k = \frac{1}{2}M^k(\epsilon^k)^2$. It can be decomposed into the contributions of each bond: $M^k = \sum_i M_i^k$. M_i^k is related to T_i^k as follows:

$$U_{j}^{k} = \frac{1}{2}M_{j}^{k}(\epsilon^{k})^{2} = \frac{1}{2}T_{j}^{k}\gamma_{j}^{k}.$$
 (2)

For a linear spring, T_j and γ_j only differ by a factor of the spring constant. This gives the following:

$$M_j^k \propto \left(T_j^k\right)^2. \tag{3}$$

 M_i^k is the contribution of bond j to M^k , where M^k is the modulus for the deformation ϵ^k . In Sec. IV it will be shown that M_i^k is a quantity that can be measured experimentally. Moreover, it is easier to measure M_j^k than to measure T_j^k or γ_i^k . Since the goal is to be able to prune the networks in experiments, the pruning protocols presented below will be based on measurements of M_i^k .

Pruning algorithm

In order to incorporate an allosteric response, it is not particularly important how much energy is required to move the source nodes apart as long as it results in an effect of the correct sign and magnitude at the target site. Therefore the individual values of (T_j^{source}) and (T_j^{target}) are of little importance; the important quantity is the product of the two, $(T_i^{\text{source}})(T_i^{\text{target}})$. This term identifies which bonds are most relevant to both source and target, and pruning the bonds with the largest $(T_i^{\text{source}} T_i^{\text{target}})$ helps create an interaction between the source and target sites.

Consider applying the input strain at source and output strain at target. The force on bond j resulting from applying both the strains together is represented as T^{s+t} :

$$T_j^{s+t} = T_j^{\text{source}} + T_j^{\text{target}}. (4)$$

Similarly, applying the input strain at *source* and the negative of output strain at *target* is represented by T^{s-t} :

$$T_j^{s-t} = T_j^{\text{source}} - T_j^{\text{target}}. (5)$$

The moduli M_j can be expressed in terms of T_j :

$$M_j^{s+t} \propto (T_j^{s+t})^2 = (T_j^{\text{source}} + T_j^{\text{target}})^2,$$
 (6)

$$M_i^{s-t} \propto (T_i^{\text{source}} - T_i^{\text{target}})^2,$$
 (7)

and

$$M_j^{\text{link}} \equiv M_j^{s+t} - M_j^{s-t} = 4(T_j^{\text{source}})(T_j^{\text{target}}).$$
 (8)

Note that taking the difference of the in-phase and out-ofphase terms produces the product of tensions due to applied strain at source and target sites. This term, M^{link} , links the effects of strains at both source and target and can be either positive or negative. One pruning protocol that would create an allosteric interaction between the source and target would be to prune those bonds in the network that have a maximum value of M^{link} .

Because $M_i^{\text{link}} = 4(T_i^{\text{source}})(T_i^{\text{target}})$ is symmetric between source and target, the source and the target have been treated on an equal footing. If this were the only criterion for pruning bonds, then the effect on the target by activating the source would be the same as the effect on the source by activating the target. Thus such a criterion would produce $\eta \approx 1$.

However, in many situations it might be preferable to have $\eta \neq 1$. For example, one might want to create a strain at the target that is twice as large as the strain at the source (i.e., $\eta = 2$). This would require that the symmetry between source and target be broken so that, for example, the target nodes are easier to move than the source nodes. One effective way to break the symmetry is to bias the modulus by giving more weight to T_i^{target} than to T_j^{source} . One way to do this is to prune the bond with a maximum value of $(M_i^{link})(M_i^{target})^n$ where

These combinations of moduli are referred to as the effective modulus, M^{eff} . In the results presented in the next section below there are three examples:

- (1) $(M^{eff,0}) = M^{\text{link}},$ (2) $(M^{eff,1}) = M^{\text{link}}M^{\text{target}}.$
- (3) $(M^{eff,3}) = M^{link} (M^{target})^3$

Our pruning algorithm is as follows:

- (1) Calculate M_i^{eff} for each bond j in the network;
- (2) Remove the bond with the maximum value of M_i^{eff} ;
- (3) Calculate the new value of η ;
- (4) Repeat until the desired value of η is obtained.

By using effective moduli as the underlying quantity that controls a network's behavior, it is possible to incorporate responses in disordered networks using local rules alone. Local rules refer to the fact that one only needs to measure the value of M_i^{eff} at each bond instead of measuring any kind of global parameter for the network. I explore the above three M^{eff} s, with n = 0, 1, 3 as representative moduli to show the effect of symmetry breaking. Appendix A shows detailed results from simulations that show the general trend as a function of n. The rest of this paper explores the efficacy of this pruning approach using spring-network simulations followed by an experimental method to measure M^{eff} in order to incorporate allosteric responses in situ in physical systems.

III. SIMULATION RESULTS

In order to check the efficacy of these algorithms, I simulate the response of networks as the protocols are applied. The simulations can be performed on networks with periodic boundaries as well as ones with free boundaries. A free boundary network is created by cropping out a circular section from a periodic network. This often produces dangling bonds or zero modes which are eliminated by removing the relevant bonds and nodes from the edges of the cropped network. Since open boundary networks are easier to build in experiments, I use these networks to compare the response between simulations and experiments.

The simulation results shown here are performed on networks that have periodic boundaries with $\sim \! 500$ particles and $\sim \! 1080$ bonds. Unpruned networks have $\eta \approx 0.0$ on average between randomly chosen source and target sites. Networks are pruned until the desired value of η is reached or until the process fails due to the creation of a zero mode in the system. 50 different networks are pruned for both positive and negative values of η . The networks used in these simulations have an average $\Delta Z = Z - Z_c \approx 0.32$. This corresponds to an excess of $\sim \! 7\%$ bonds more than necessary to maintain rigidity.

The pruning algorithms themselves do not depend on the desired value of η . As a network is pruned, $|\eta|$ increases steadily until it exceeds the specified value of $|\eta|$. The pruned networks never have a response that is exactly equal to the desired η , and the network is considered to be successfully pruned when the desired value of $|\eta|$ is first exceeded. The success rate of each of the pruning methods is shown in Fig. 1(b). As one might expect, if we prune for higher $|\eta|$, the success rate decreases. It is clear from this data that using just M^{link} to prune a network is not the best strategy because, due to the symmetry between source and target, one can prune only to a maximum of $|\eta| \approx 1$. Even this response can be achieved only about half the time.

Biasing $M^{\rm eff}$ towards the target improves the effectiveness of pruning significantly; using $M^{\rm eff,3} = (M^{\rm link})(M^{\rm target})^3$ makes it possible to reach $|\eta| > 1000$. However, it is important to note that these calculations are performed in the linear-response regime of the network. Such a very large $|\eta|$ implies that the source strain must be extremely small in order for the target strain to be 1000 times the source strain and still be in the linear regime. This makes it highly impractical to measure such a response in a laboratory system.

These results are from networks with periodic boundaries, but the trend remains the same for networks with open boundaries. The exact values of success rates depends on other factors such as the distance between source and target sites. For a given system size, it is generally easier to prune a network where source and target are closer together.

Figure 1(c) shows the average fraction of bonds that need to be pruned as a function of η . We see that 100% of the networks fail after an average of \sim 6% bonds are removed. This is when nearly all the excess bonds above the rigidity threshold have been removed; therefore removing any subsequent bond has a high probability of creating a zero-energy mode.

Efficiency in experiments

It is known from previous studies that linear spring simulations do not capture all the material details of a real network [7,12]. There are other interactions, such as angle-bending forces, that are present in a real material. In order to test how well our pruning algorithms translate to real networks, we design 2D networks with open boundaries using the three mentioned protocols and then fabricate them in experiments.

We took networks with free boundaries ranging between 110 and 150 particles in size and pruned each of them using our three protocols. We stopped pruning either once the network achieved $\eta > 1$ or once a zero mode was produced so that the pruning process failed. Since not all of our algorithms

have a 100% success rate, we chose 10 networks that could be pruned successfully using the three effective moduli, $(M^{eff,0})$, $(M^{eff,1})$, and $(M^{eff,3})$. For consistency, in all three cases the same set of source and target nodes are used. For any given starting network, each protocol removes a different set of bonds. I then laser cut 30 realizations of these networks (10 networks \times 3 algorithms) and measured their responses in experiments.

Our networks were laser cut from 1.5-mm-thick sheets of silicone rubber with a hardness of shore A70. The bonds were made thinner near the nodes to minimize angle-bending interactions in the networks as was done in previous work [4]. The ratio of the width of a bond to its average length is 1:6, with the bonds being half as wide near the nodes.

The observed η of these laser-cut networks is measured by applying an input strain of 5% at the source and measuring the output strain at the target site. Figure 1(d) shows the response of these networks. In order to measure how well a network pruned in simulations responds in experiments, the experimental result for each network, η_{exp} , is normalized by the value of η produced in the simulation, η_{sim} : $\mathcal{R} = \eta_{exp}/\eta_{sim}$. The fraction of networks whose response exceeds a given \mathcal{R} is plotted as a function of \mathcal{R} . Note that this is the only time the success rate needs to be measured as a function of \mathcal{R} instead of η . If our simulations were a perfect model for the experimental systems, then the data in Fig. 1(d) would have been a horizontal line at 1.0.

This data is surprising, because some algorithms have much better agreement between experiments and simulations than others. Interestingly, Fig. 1(b) shows that pruning with $M^{eff,0} = M^{\text{link}}$ works only about 50% of the time, but when these networks are translated to experiments, they have a very high success rate. On the other hand, $M^{eff,3} = M^{\text{link}}(M^{\text{target}})^3$ works very well in simulations but not in experiments. This suggests that the disparity between experiments and simulations increases as the complexity of the pruning algorithm increases. I hypothesize that the inclusion of $(M^{\text{target}})^n$ increases the effect of the nonlinear terms so that the predictions from simulation are farther from our experimental results.

IV. PRUNING in situ

Our results show that linear spring models do not work perfectly for designing real materials. In order to see what is going on in the laboratory material, we need a way to measure the stresses in a physical network. This section presents experiments to measure the stress distribution in physical networks and use that information to prune the networks *in situ*.

Setup

The stresses in a transparent material can be quantitatively detected by measuring stress-induced birefringence [13]. The linear polarization of a beam of light will not be affected as it passes through an isotropic material; an analyzing polarizer with perpendicular orientation on the exiting side of the material will block all the light. A photographic image would be completely dark. However, if there are stresses in the photoelastic material, the polarization axis of the light will be rotated depending on the orientation of the stress with respect

to the polarization axis. The relative phase shift, Δ , between two principal directions is proportional to the difference in the two principal stresses [13]:

$$\Delta \propto S_1 - S_2. \tag{9}$$

If the stresses are small enough so that the rotation angle is small, the analyzing polarizer will transmit the light in proportion to the stress. A photographic image will be bright in those regions where the stress is large and completely dark where there is no net stress. In the simplified spring-network model, the only nonzero stress is along the length of the bond. In a physical network, there could be forces along any direction in the material. Using circularly polarized light allows the total magnitude of the stress to be measured regardless of its orientation. The drawback of using circular polarization is that circular polarizers are sensitive to the wavelength of the light. Thus monochromatic light must be used.

In the experimental measurements of stresses reported here, the disordered networks are made out of molded urethane rubber (Smooth-on Clear Flex 50) with a shore hardness of A50. This material is highly sensitive to stresses and allows measurement of stresses in the range of 4–20 kPa in the current setup. The liquid urethane material is poured into molds in the shape of the desired networks. The molds are 3D printed in a soft rubber material with a shore hardness of A28. Before each use, the molds were coated with a release agent (EaseRelease 200) to ensure that the molded urethane networks are easy to remove from the molds. The networks were cured in the mold at room temperature for a duration of 12 h. After removal from the mold, they were cured for an additional 2–3 days at room temperature to reduce the tackiness of the surfaces of the molded networks.

A schematic of the experimental setup is shown in Fig. 2(a). Data is collected by the camera at wavelength $\lambda = 500 \pm 10\,nm$. The initially unpolarized white light is first polarized using a linear polarizer and then converted to circular polarization using a quarter-wave plate for $\lambda = 500\,nm$. The light then passes through the sample. On the other side of the sample, another quarter-wave plate converts the light back to linearly polarized light followed by a linear polarizer that is oriented perpendicular to the polarization of the initial light. The total stress at each point in the material can be measured by the intensity of the light in the photographic image.

Even after letting the molded photoelastic networks cure for a few days, their surfaces are still tacky enough to stick to a glass or acrylic surface. This produces extraneous stresses in the material that are unrelated to those caused simply by placing strains at the source or target nodes. Additionally, because of a high surface tension of the molding liquid, the top surface of the network has a meniscus so that it is not completely flat. As a result, a ray of light going through such a curved surface is reflected and refracted in various directions and gives rise to unwanted signals in our data.

Both of these problems can be eliminated by submerging the networks in an index-matched fluid. I used mineral oil with a refractive index of 1.47, which is very close to the refractive index of the photoelastic networks, which is 1.48. Sample images from this setup with and without an applied strain are shown in Figs. 2(b) and 2(c), respectively. The image in

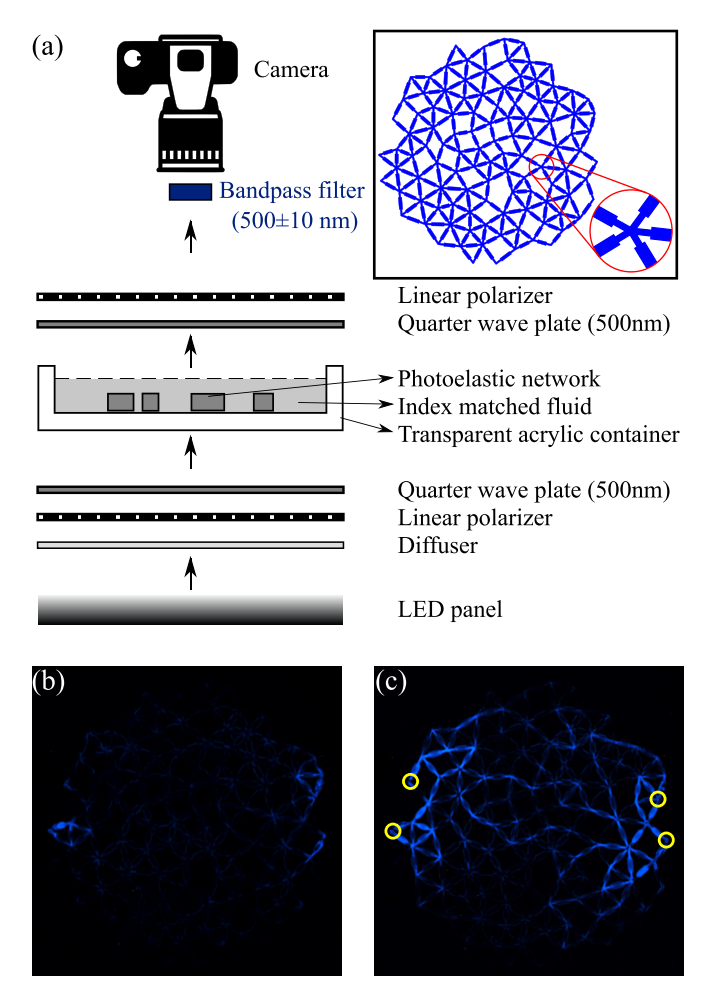


FIG. 2. (a) Setup for visualizing stresses in photoelastic networks including a design of a sample photoelastic network. Zoomed-in picture shows the variation of bond width near a node. (b) Same network as above cast out a photoelastic material imaged in the experimental setup with no external strain. (c) Image of the same network as in (b) with applied strains between adjacent node pairs circled in yellow.

Fig. 2(b) shows that when the network is under no stress, the image of the network in the camera is dark and nearly undetectable.

When an external strain is applied to the network as shown in Fig. 2(c), different bonds in the network are stressed by different amounts as a reaction to the input strain. These stressed regions now appear as bright spots in our image.

The intensity of light, I(x, y), at any point in the material (x, y) is related to the electric field, E(x, y), and the phase shift, $\Delta(x, y)$:

$$I(x, y) \propto E(x, y)^2 \propto \sin[\Delta(x, y)]^2 \propto \sin[S(x, y)]^2$$
. (10)

As long as the input strain is sufficiently small, the resultant stresses are in the regime where $\sin(S) \approx S$. In this limit, the brightness of a bond is proportional to the square of stress. Hence the intensity I averaged over the length of bond j is proportional to M_j in Eq. (3).

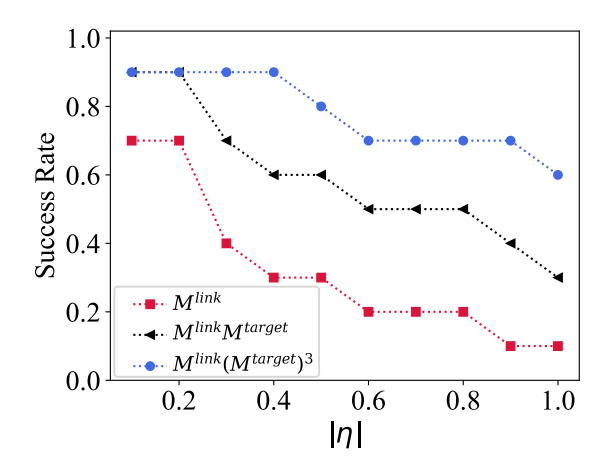


FIG. 3. Success rate of networks pruned *in situ* as a function of η . Following the same trend as the simulations, networks pruned to lower the effective moduli $M^{\rm eff} = M^{\rm link} (M^{\rm target})^3$ (blue circles) have the highest success rate, followed by $M^{\rm eff} = M^{\rm link} M^{\rm target}$ (black triangles) and $M^{\rm eff} = M^{\rm link}$ (red squares).

Experimental results

I conduct the *in situ* pruning experiments on photoelastic networks that are between 110 and 150 nodes in size. The photoelastic networks are molded to be 5 mm thick with an average bond length of 12 mm. The ratio of the width of a bond to its average length is 1:4, with the bonds being a third as wide near the nodes than in their middle. This slight difference in geometry makes the middle part of the bonds wider than in the experiments described above that pruned bonds according to the algorithm based on simulation results. It ensures that the effect of noise from the edges of photoelastic bonds is minimized. In order to measure the response of these pruned networks, I remake them in silicone rubber using the same specifications as in Sec. III. This is done to avoid any differences arising from the material properties while comparing the response of designed and experimentally pruned networks.

In order to prune these networks, I take images where a strain is applied (i) at the source and target in phase (M^{s+t}) , (ii) out of phase (M^{s-t}) , and (iii) only at the target site (M^{target}) . By computing combinations of these images, I obtain a measure of the same three effective moduli as defined in Sec. II: $M^{\text{eff}} = M^{\text{link}}$, $M^{\text{eff}} = M^{\text{link}}M^{\text{target}}$, and $M^{\text{eff}} = M^{\text{link}}(M^{\text{target}})^3$. The experiments were conducted on 10 different networks for each M^{eff} . In each pruning step, I first calculate M^{eff} for all the bonds, remove the bond with maximum M^{eff} , and then measure η of the pruned network. As the bonds are pruned sequentially, the signal-to-noise ratio drops steadily; when the signal is too low to be reliable, the pruning is halted. The recorded η for a particular sample is the maximum η that the network exhibits at any point during the pruning process.

The results from *in situ* pruning experiments are shown in Fig. 3. To some extent, all pruning methods show an allosteric response. In particular, by sequentially removing the bond with the largest value of $M^{eff,3} = M^{link}(M^{target})^3$ at each step, networks can often be successfully pruned to produce $\eta = 1$. The three different pruning methods have very different

success rates. This was also seen in the simulation results shown in Fig. 1(b). The results from the experiments and from the simulations follow the same trend. The maximum η to which a network can be pruned depends on the system size. Smaller networks can generally be pruned to higher values of η . For a particular network design, the exact value of η depends on various factors including the network material and the geometry of the bonds. It has been previously shown that η can be varied by modifying the width of the bonds near the nodes [4].

The same network design pruned to minimize the same $M^{\rm eff}$ leads to the removal of very different sets of bonds in simulations versus those pruned in the photoelastic experiments. This is not surprising, since the simulations only considered central harmonic springs, whereas the experiments had all the interactions inherent in an elastic sheet, such as angle-bending forces at each node and nonlinear stress/strain curves for all the bonds. This can be seen clearly by comparing Fig. 3 and Fig. 1(d). Both of these plots show how well the networks perform in experiments when they have been pruned using three different M^{eff} s. The only difference being that in Fig. 1(d), the stresses are measured in spring-network simulations, and in Fig. 3, the stresses are measured experimentally. However, it is surprising that, compared to the experimental results shown in Fig. 1(d), the trend for networks pruned in situ is completely reversed. This suggests that the simulation models are too simple to capture all the stresses in a real

One limitation of the data presented in Fig. 3 is that most networks could not be pruned to $\eta > 1$. However, the exact value of η that can be incorporated in a network depends on various factors, including system size, material properties, and network geometry. By modifying one or more of these parameters, one could design networks with higher values of η .

These results reinforce the conclusion that in order to make a physical system with an allosteric response, a simplified model is not sufficient and it is important to visualize and measure all the interactions in the system. Using an experimental procedure to detect the stresses in physical networks, it is possible to create allosteric networks in experiments with a high success rate.

V. CONCLUSIONS

The emphasis of this work has been to understand the local pruning rules that control allosteric response in mechanical networks as well as to fabricate these networks in real (physical) experimental systems. In order to create a robust response, it is important to identify the relevant parameters that govern allosteric behavior. The effective moduli introduced here are the bond-level contributions to allostery. The simulations show that this approach is very effective at designing allosteric responses with minimal computational cost. In some cases, the results of these simulations can be directly translated into experimental realizations. These local pruning rules are more efficient than previous methods for incorporating allosteric behavior into experimental systems [4]. Similar local pruning rules can also be used to create more general responses, such as multiple pairs of allosteric source and target sites, or a single source site controlling multiple target sites. Predictably, when the complexity of the incorporated response increases, the efficiency of such pruning algorithms goes down.

As expected, however, the simulations of networks connected by linear, central-force springs do not capture all the details of a real material. In order to create allosteric responses efficiently in experiments, it is necessary to be able to measure stress distributions in the physical networks. I have presented an experimental procedure to visualize and measure the stresses in these systems and use them to prune the appropriate bonds in the networks *in situ* to achieve a desired response.

The experimental technique to measure local stresses provides a pathway for modifying physical systems with more complex interactions. It would be interesting to see if it can be used to create other mechanical responses, such as auxetic behavior. This protocol can also be applied to other disordered systems that are not based on spring networks. The anisotropy in stress distributions in these networks is reminiscent of the anisotropy in contact forces in jammed packings [14]. The pruning methods explored here could be extended to 3D systems and to smaller length scales by using stimuli responsive materials that can detect stresses in polymers at the molecular level [15,16].

Recent work has shown that stress-induced aging can be used to modify material properties [17]. An externally imposed strain can *direct* the evolution of a material and determine its mechanical response. Our understanding of local pruning rules that control allostery in combination with directed aging protocols can be very useful in designing allosteric systems while eliminating the need to manipulate the material manually at the microscopic level. Local learning rules, such as those presented here, are also of interest in supervised learning of elastic and flow networks [18]

In conclusion, local pruning rules that allow the manipulation of material response combined with the ability to measure stress distributions *in situ* enable the modification of materials that are more complex than the linear spring networks that have been the focus of previous simulation studies. This approach opens up ways to build mechanical metamaterials with a desired function without relying on computer simulations.

ACKNOWLEDGMENTS

I would like to thank D. Hexner, A. J. Liu, and N. Stern for insightful discussions. I am deeply grateful to S. R. Nagel for his advising and mentoring. I would also like to thank C. S. Bester for information regarding photoelastic materials and R. Morton for help with 3D printing. This work was supported by the NSF MRSEC Program DMR-2011854 (for experimental studies), the US Department of Energy, Office of Science, Basic Energy Sciences, under Grant No. DE-SC0020972 (for theoretical model development and simulations).

APPENDIX A: EFFECT OF SYMMETRY BREAKING ON SUCCESS RATE

The difference between various pruning protocols explored in this paper is the inclusion of the term $(M_j^{\text{target}})^n$ that breaks the symmetry. Above I focused on three examples: n = 0, 1,

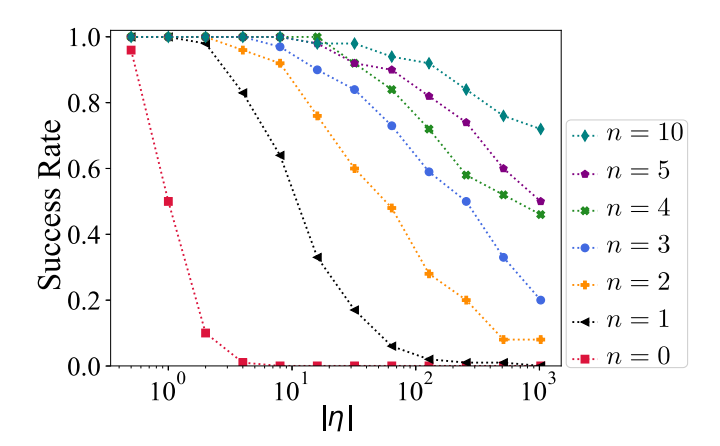


FIG. 4. Success rate of networks pruned in simulations as a function of $|\eta|$. Networks pruned to lower the effective moduli $M^{\text{eff}} = M^{\text{link}}(M^{\text{target}})^n$ with n ranging from 0 to 10.

and 3. In Fig. 4 I show the comparison between the success rate for a range of n. This plot shows that as the effective moduli $M^{\rm eff}$ is increasingly biased towards $M^{\rm target}$, the success rate also increases monotonically. For $\eta = \mathcal{O}(1)$, a small bias towards $M^{\rm target}$ is sufficient to successfully prune the network nearly 100% of the time. For $\eta \gg 1$, a greater bias is needed to produce a high success rate.

APPENDIX B: COMPUTING BOND-LEVEL RESPONSE

The tensions and moduli of individual bonds are obtained by calculating the linear response of spring networks. This section follows the notation used in previous work in the literature [19]. Consider a system with N_b bonds and N nodes in d dimensions. The tensions and elongations in the bonds are represented as vectors $|t\rangle$ and $|e\rangle$, respectively, each with length N_b . In the simulations presented in this work, an external tension $|t^*\rangle$ is applied and the system is allowed to equilibrate in response to $|t^*\rangle$. The resultant $|t\rangle$ and $|e\rangle$ respectively give the tension and extension of the whole system. The resultant tension on bond j, referred to in this work as T_j , is simply the jth component of the tension vector $|t\rangle$.

In order to calculate the network response, one needs the compatibility matrix (C) and the flexibility matrix (F). The compatibility matrix (C) is a rectangular, $N_b \times dN$ matrix that has all the information about the position of nodes and connectivity of bonds in a network under mechanical equilibrium with no external forces. The flexibility matrix (F) is a diagonal $N_b \times N_b$ matrix that gives the stiffness of each bond and is defined as

$$\langle i|F|j\rangle = \frac{\delta_{ij}}{k_i},$$
 (B1)

where k_i is the spring constant of bond i. In this work, k_i is set to be σ/l_i , where σ sets the material stiffness and has units of energy per unit length, and l_i is the length of bond i. Tension and extension vectors are related to each other according to Hooke's law:

$$|t\rangle = F^{-1}|e\rangle. \tag{B2}$$

The dynamical matrix, $D = C^T F^{-1}C$, is a square $dN \times dN$ matrix that computes the equilibrium configuration of the

system. The resultant bond extensions are related to the externally applied tension as follows:

$$|e\rangle = CD^{-1}C^T|t^*\rangle.$$
 (B3)

The pruning algorithms used in this paper are based on measurements of individual bond contributions to moduli M^*

for various externally applied deformations. M_j^* is the contribution of bond j to M^* and can be calculated for any applied tension $|t^*\rangle$ using the resultant tensions $|t\rangle$ and extensions $|e\rangle$:

$$M_i^* = \frac{1}{2} \langle e||j\rangle \langle j||t\rangle. \tag{B4}$$

- C. P. Goodrich, A. J. Liu, and S. R. Nagel, The Principle of Independent Bond-Level Response: Tuning by Pruning to Exploit Disorder for Global Behavior, Phys. Rev. Lett. 114, 225501 (2015).
- [2] D. Hexner, A. J. Liu, and S. R. Nagel, Role of local response in manipulating the elastic properties of disordered solids by bond removal, Soft Matter 14, 312 (2018).
- [3] D. Hexner, A. J. Liu, and S. R. Nagel, Linking microscopic and macroscopic response in disordered solids, Phys. Rev. E **97**, 063001 (2018).
- [4] J. W. Rocks, N. Pashine, I. Bischofberger, C. P. Goodrich, A. J. Liu, and S. R. Nagel, Designing allostery-inspired response in mechanical networks, Proc. Natl. Acad. Sci. 114, 2520 (2017).
- [5] L. Yan, R. Ravasio, C. Brito, and M. Wyart, Architecture and coevolution of allosteric materials, Proc. Natl. Acad. Sci. 114, 2526 (2017).
- [6] T. Tlusty, A. Libchaber, and J.-P. Eckmann, Physical Model of the Genotype-to-Phenotype Map of Proteins, Phys. Rev. X 7, 021037 (2017).
- [7] D. R. Reid, N. Pashine, J. M. Wozniak, H. M. Jaeger, A. J. Liu, S. R. Nagel, and J. J. de Pablo, Auxetic metamaterials from disordered networks, Proc. Natl. Acad. Sci. 115, E1384 (2018).
- [8] J. W. Rocks, H. Ronellenfitsch, A. J. Liu, S. R. Nagel, and E. Katifori, Limits of multifunctionality in tunable networks, Proc. Natl. Acad. Sci. 116, 2506 (2019).
- [9] A. J. Liu and S. R. Nagel, The jamming transition and the marginally jammed solid, Annu. Rev. Condens. Matter Phys. 1, 347 (2010).

- [10] W. G. Ellenbroek, V. F. Hagh, A. Kumar, M. F. Thorpe, and M. van Hecke, Rigidity Loss in Disordered Systems: Three Scenarios, Phys. Rev. Lett. 114, 135501 (2015).
- [11] C. S. O'Hern, L. E. Silbert, A. J. Liu, and S. R. Nagel, Jamming at zero temperature and zero applied stress: The epitome of disorder, Phys. Rev. E 68, 011306 (2003).
- [12] D. R. Reid, N. Pashine, A. S. Bowen, S. R. Nagel, and J. J. de Pablo, Ideal isotropic auxetic networks from random networks, Soft Matter 15, 8084 (2019).
- [13] E. Hecht, Optics, 4e (Addison-Wesley, Reading, MA, 2002).
- [14] N. Brodu, J. A. Dijksman, and R. P. Behringer, Spanning the scales of granular materials through microscopic force imaging, Nat. Commun. 6, 6361 (2015).
- [15] Y. Chen, C. J. Yeh, Y. Qi, R. Long, and C. Creton, From force-responsive molecules to quantifying and mapping stresses in soft materials, Sci. Adv. 6, eaaz5093 (2020).
- [16] N. Deneke, M. L. Rencheck, and C. S. Davis, An engineer's introduction to mechanophores, Soft Matter 16, 6230 (2020).
- [17] N. Pashine, D. Hexner, A. J. Liu, and S. R. Nagel, Directed aging, memory, and nature's greed, Sci. Adv. 5, eaax4215 (2019).
- [18] M. Stern, D. Hexner, J. W. Rocks, and A. J. Liu, Supervised Learning in Physical Networks: From Machine Learning to Learning Machines, Phys. Rev. X 11, 021045 (2021).
- [19] T. C. Lubensky, C. L. Kane, X. Mao, A. Souslov, and K. Sun, Phonons and elasticity in critically coordinated lattices, Rep. Prog. Phys. 78, 073901 (2015).